Journal of Statistical Physics, Vol. 62, Nos. 5/6, 1991

Neutron Scattering Studies of Molecular Conformations in Liquid Crystal Polymers

L. Noirez,[1] F. Moussa,[1] J. P. Cotton,[1] P. Keller, and G. Pépy[1]

Received October 27, 1989; final April 25, 1990

A comblike liquid crystal polymer (LPC) is a polymer on which mesogenic molecules have been grafted. It exhibits a succession of liquid crystal phases. Usually the equilibrium conformation of an ordinary polymeric chain corresponds to a maximum entropy, i.e., to an isotropic spherical coil. How does the backbone of a LCP behave in the nematic and smectic field? Small-angle neutron scattering may answer this question. Such measurements are presented here on four different polymers as a function of temperature. An anisotropy of the backbone conformation is found in all these studied compounds, much more pronounced in the smectic phase than in the nematic phase: the backbone spreads more or less perpendicularly to its hanging cores. A comparison with existing theories and a discussion of these results is outlined.

KEY WORDS: Conformations of polymers; small-angle neutron scattering; liquid crystal structures; polymers; transitions of liquid crystals.

1. INTRODUCTION

During the recent years, liquid crystal polymers have given rise to a great interest in theoretical, experimental, and applied physics. Indeed, these compounds have the properties of liquid crystals associated to usual properties of polymers.(1)

Let us recall that a polymer is the result of the repetition of a given molecular unit. In the melt state, its equilibrium conformation corresponds to the maximum entropy. In the bulk it has the shape of an isotropic coil, the characteristic size of which is proportional to the root square of its total length.(2)

---

[1] Laboratoire Léon Brillouin (CEA-CNRS), CEN-Saclay, 91191 Gif-sur-Yvette Cedex, France.

Liquid crystal compounds exhibit intermediate partially ordered states between the conventional solid phase and isotropic liquid phase. The anisotropic molecules of such compounds, like small rods, have their long axis parallel to each other without any long-range translational order in the nematic phase, while, in the smectic phase, the molecules are stacked in smectic layers with well-defined thickness (Fig. 1).(3)

A liquid crystal polymer (LCP) is a polymer on which has been grafted short molecules showing liquid crystal phases. There are two kinds of LCP, following the place where mesogens are inserted: main-chain LCP are polymers where mesogenic cores are included in the chain; side-chain LCP are polymers where mesogenic moieties are laterally hanging like teeth of a comb (Fig. 2). These latter compounds have at the same time interesting technological properties (see ref. 1 and the present issue) (e.g., they allow a very good aligment of ions in a matrix useful for nonlinear optical devices, they have strong mechanical resistance,...) and interesting physical and fundamental properties. Indeed, on the one hand, the backbone, as in usual polymers, tends to be in an isotropic conformation, a source of maximum entropy, and on the other hand, it undergoes liquid crystal order from its own mesogens. So an interesting question is: What will be the result of this competition on the backbone conformation? Neutron scattering experiments associated to the labeling method are good means to measure the conformation of a polymer. The results of this technique applied to several LCP are reviewed in this paper. They are compared to predictions of existing theories.

This paper is organized as follows. In the next section we present experimental techniques and the results we have obtained. In Section 3 a brief review of existing theories on LCP is introduced. In Section 4 a comparison between theories and experiments is tentatively made and some conclusions are given.

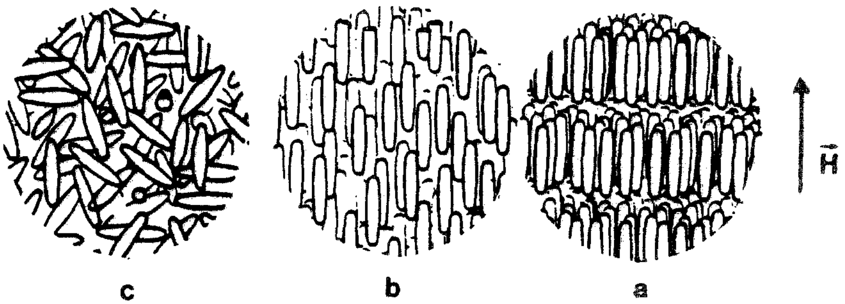

Fig. 1. Liquid crystal phases: (a) smectic phase, (b) nematic phase, (c) isotropic liquid phase. Note the magnetic field H, which aligns the long axis of mesogenic molecules.

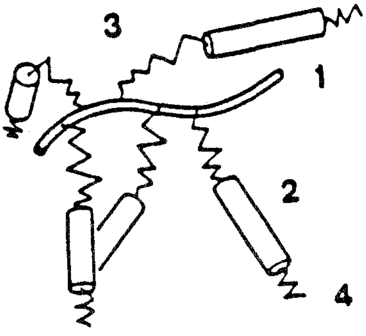

Fig. 2. Liquid crystal polymer: 1, backbone; 2, mesogenic core; 3, spacer; 4, terminal group.

2. NEUTRON SCATTERING EXPERIMENTS

2.1. The Labeling Method

The labeling method is based on selective deuteration, associated to small-angle neutron scattering, and allows one to determine the conformation of the backbone of LCP in the bulk. The neutron scattering cross section is defined as follows:

$$S(\mathbf{q}) = \sum_{i,j} a_i a_j \exp(i\mathbf{q} \cdot (\mathbf{r}_i - \mathbf{r}_j))$$

where $\mathbf{r}_i$ and $\mathbf{r}_j$ are the positions of atoms i and j in the polymers at the same time, and a_i and a_j are their respective scattering amplitudes. $\mathbf{q}$ is the scattering wave vector, i.e., the momentum transfer of neutrons: $\mathbf{q} = \mathbf{k} - \mathbf{k}_0$, where $\mathbf{k}_0$ is the wave vector of monochromatic incident neutrons and $\mathbf{k}_0$ the wave vector of scattered neutrons. The scattering angle θ is $\theta = (\mathbf{k}_0, \mathbf{k})$; then $|\mathbf{q}|$ reads

$$|q| = [4\pi \sin(\theta/2)]/\lambda \qquad \text{with} \quad |\mathbf{k}| = |\mathbf{k}_0| = 2\pi/\lambda$$

The neutron scattering function $S(q)$ at small q values gives information of a macroscopic kind on the sample. It is well known$^{(4)}$ that if the sample is homogeneous, $S(q) \to 0$ with $q \to 0$. If it is not, the analysis of $S(q)$ gives characteristic sizes of inhomogeneities. A good means to create heterogeneity in polymers is to make a mixture of protonated compounds and selectively deuterated compounds. It can be shown$^{(4)}$ that the scattering function of a sample with a molecular concentration of protonated polymers x_H and a concentration of deuterated polymers x_D ($x_H + x_D = 1$) is given by

$$S(q) = N x_H x_D (a_H - a_D)^2 P(q) \tag{1}$$

N is the total number of polymer chains, a_D, a_H are coherent neutron scattering amplitudes of protonated and deuterated monomers, $(a_H - a_D)^2$ is the contrast term, which can be very important for neutron scattering, and $P(q)$ is the form factor of one chain defined by

$$P(q) = \left\langle \sum_{i,j}^{n,n} \exp[iq \cdot (r_i - r_j)] \right\rangle \tag{2}$$

This sum is made on a single polymeric chain with n repetitive units (n is the degree of polymerization), and r_i describes the position of the ith monomer in the chain. The average is taken over all the possible conformations of the polymer. From expression (1) it is clear that $S(q)$ is maximum for $x = 0.5$, which is why all measurements were done on samples with this value of concentration. Note that in the so-called deuterated compounds only the backbone is deuterated (Fig. 3), so $P(q)$ is directly related to the radius of gyration of the backbone R_g defined as follows:

$$nR_g^2 = \sum_{i=1}^{n} \langle r_i^2 \rangle \tag{3}$$

It can be shown that the scattered neutron intensity $I(q)$, in the frame of Zimm's approximation in the Guinier range[5] defined by

$$q \leqslant 1/R_g \tag{4}$$

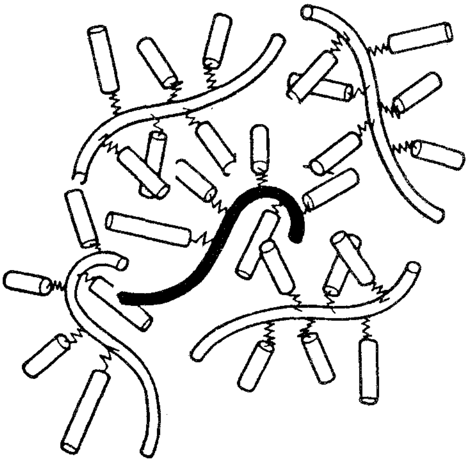

Fig. 3. A deuterated backbone with its hanging molecules among protonated LCP.

can be written as

$$1/I(q) = 1/I(0)(1 + 1/3q^2R_g^2) \tag{5}$$

So, under the condition (4) and the assumption of isotropic conformation, the radius of gyration is directly deduced from the slope of a straight line in a representation of the inverse of intensity as a function of the square wave vector.

If the conformation of the backbone is no longer isotropic, three components of radius of gyration can be defined:

$$nR_{gl}^2 = \sum_{i=1}^{n} \langle r_{il}^2 \rangle \qquad \text{with} \quad l = x, y, z$$

Then the form factor reads

$$P(q) \approx n^2(1 - q_x^2R_{gx}^2 - q_y^2R_{gy}^2 - q_z^2R_{gz}^2) \tag{6}$$

q_x, q_y, q_z are the three components of wave vector q. With a two-dimensional (2D) multidetector, one is able to measure R_{gx} and R_{gy}. If Ox is the axis parallel to the magnetic field which aligns mesogenic molecules, R_{gx} is called $R_{\parallel}$: it is the component of radius of gyration of the backbone parallel to the long axis of the hanging mesogenic molecules. R_{gy} is the component perpendicular to the mesogens; it is named $R_{\perp}$. So, if the conformation of the backbone of LCP is isotropic in the plane Oy, Oz, one will measure only two different components:

$$R_{gy} = R_{gz} = R_{\perp} \qquad \text{and} \qquad R_{gx} = R_{\parallel}$$

The radius of gyration is then given by

$$R_g^2 = 2R_{\perp}^2 + R_{\parallel}^2$$

In this case the scattered intensity measured with a 2D multidetector satisfies

$$1/I(q_x, q_y) = 1/I(0)(1 + q_x^2R_{\parallel}^2 + q_y^2R_{\perp}^2) \tag{7}$$

As an example, on Fig. 4a where the sample is aligned such that its Oy, Oz plane is parallel to the 2D multidetector, it can be seen that the scattered intensity is isotropic in the plane Oy, Oz, so it can be deduced that the polymer has an isotropic conformation in that plane. An important anisotropy is clearly evidenced in the plane q_x, q_y in Fig. 4b, where the sample is aligned such that its Ox, Oy plane is parallel to the 2D multidetector. The scattered intensity spreads along the q_x direction, so

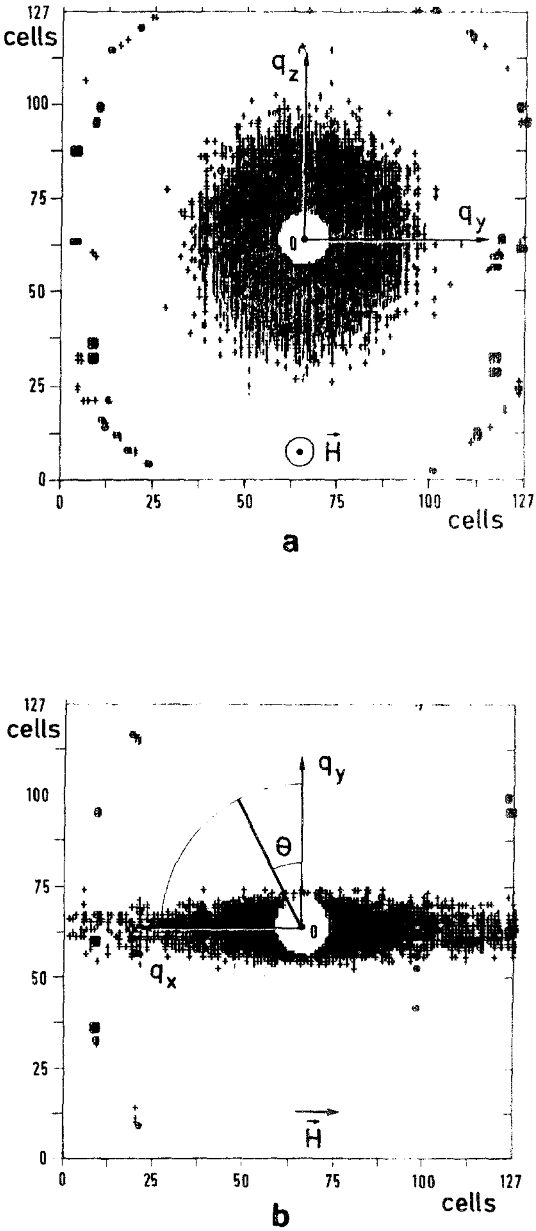

Fig. 4. (a) Isotropic scattered intensity in the plane q_y, q_z. (b) Anisotropic scattered intensity in the plane q_x, q_y [the scale of intensity is not the same as in (a)]. (c) Backbone conformation with $R_{\parallel} \ll R_{\perp}$.

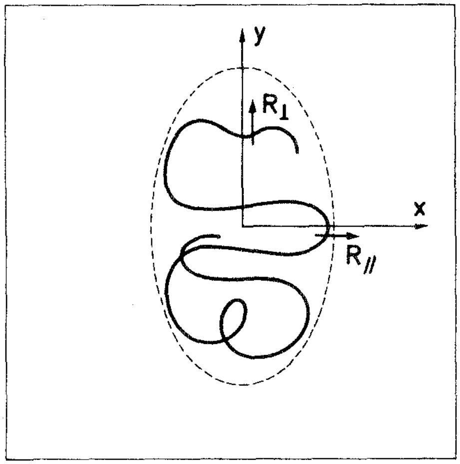

c

Fig. 4. (*Continued*)

$R_{\parallel} \ll R_{\perp}$, which means (Fig. 4c) that the polymer is rather stretched perpendicular to the magnetic field direction and to the long axis of its side mesogenic molecules.

2.2. Small-Angle Neutron Scattering (SANS) Measurements

Neutron experiments presented here have been carried out on the SANS spectrometer PAXY in the reactor ORPHEE at the Laboratoire Léon Brillouin-Saclay (Fig. 5). Details of experimental conditions are described elsewhere.(6,7) Let us just recall that a 1.4-T magnetic field aligns mesogens in the nematic phase; at lower temperatures, in the smectic phase, one controls alignment by measuring the first Bragg peak characteristic of smectic layers (Fig. 6). The range of values of wave vector where SANS is measured is

$$10^{-3} < q < 10^{-1}\ \text{Å}^{-1}$$

2.3. Results

Samples.(6) Among all the studied LCP, we present here the results on LCP with two kinds of backbone:

polyacrylate (PA):

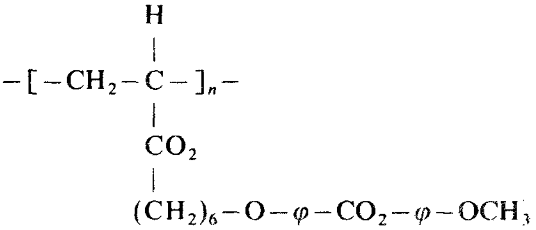

$$-[-CH_2-C(H)(CO_2-(CH_2)_6-O-\varphi-CO_2-\varphi-OCH_3)-]_n-$$

polymethacrylate (PMA):

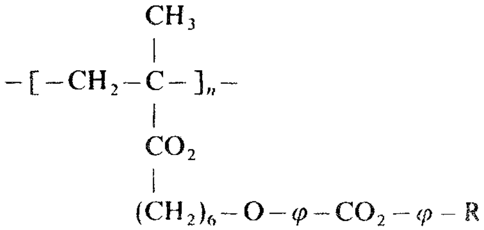

$$-[-CH_2-C(CH_3)(CO_2-(CH_2)_6-O-\varphi-CO_2-\varphi-R)-]_n-$$

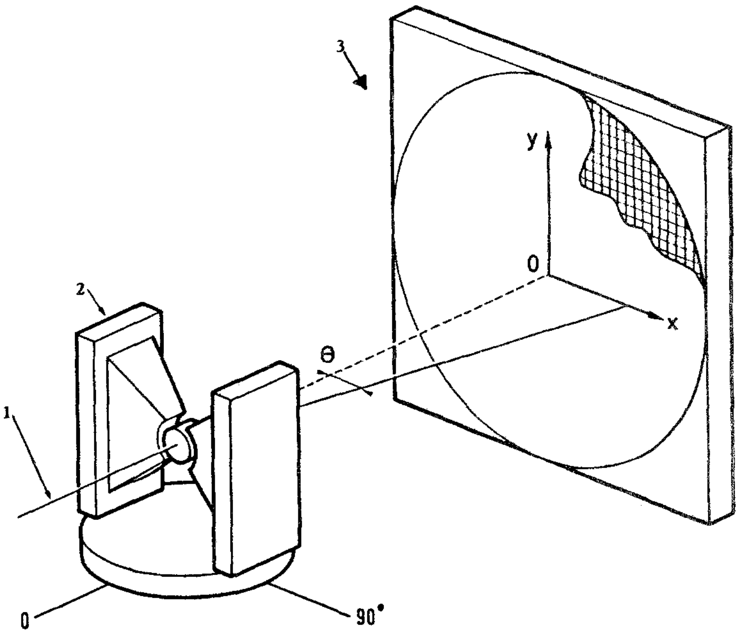

Fig. 5. Scheme of SANS spectrometer: 1, monochromatic neutron beam; 2, electromagnet field of 1.4 T in Ox direction (in the gap: sample in a furnace); 3, the 128 × 128 cell multidetector PAXY.

Spacer and mesogenic core are kept the same in all compounds (φ stands for the phenyl ring). The tail R is changed in the three different methacrylates: R is OCH_3 or OC_4H_9 or CN. Let us recall that in what we call deuterated compounds, only the backbone is deuterated. For the polyacrylate PA-OCH_3, molecular weight is of the order of 40,000, and the degree of polymerization n is of the order of 100. For polymethacrylates (PMA-OCH_3, PMA-OC_4H_9, PMA-CN), the molecular weight varies from 35,000 to 1000,000 ($270 \leqslant n \leqslant 800$). Whatever the compound, polydispersity is always between 2 and 4. The succession of mesophases for the different studied compounds is the same: liquid, nematic, smectic. The transition temperature values will be given below.

SANS Results.(6–10) Figure 6 gives an example of a measured spectrum. The scatterer sample is a 1:1 mixture of PMA-OC_4H_9 with protonated backbone and deuterated backbone in its smectic phase. The center of the beam catcher defines the origin of reciprocal space. One can see clearly that the scattered intensity near the origin is very anisotropic. The intensity spreads along the q_x direction, which is perpendicular to smectic layers, while the line shape along the q_y axis is much narrower. So

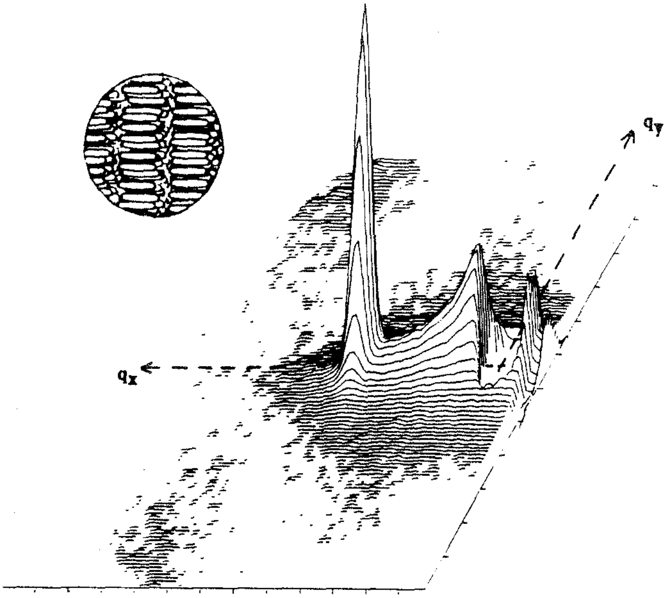

Fig. 6. Spectrum collected on the PAXY multidetector: the sample is PMA-OC_4H_9 in the smectic phase. The center of the beam catcher defines the origin of reciprocal space. Note the anisotropy of the scattered intensity around this area and the first Bragg peak position, at $2\pi/d$. On the left of the figure, LCP smectic layers are represented with their normal parallel to the Ox direction (backbones are not drawn).

it can be immediately deduced, as explained in Section 2.1, that the backbone is stretched in the direction q_y while its mean size is small along the direction of q_x:

$$R_{\parallel} \ll R_{\perp}$$

One also can observe on Fig. 6 a strong scattering at the first Bragg peak position, characteristic of the smectic order. The position of the Bragg peak gives the thickness of the smectic layers. For PMA-OC_4H_9, PMA-OCH_3, and PA-OCH_3, this thickness is equal to the length of mesogenic core of the order of 25 Å: this corresponds to a monolayered smectic phase called SmA1. Moreover, the analysis of the Bragg peak (maximum intensity and full-width at half-maximum) gives indications of the good alignment of the sample in its smectic phase. In order to get, in a spectrum, a Bragg peak (Fig. 6) whose position is about $q \approx (2\pi/25) \approx 0.25$ Å^{-1}, the wavelength of the incident neutron beam is set at $\lambda = 3.13$ Å. But, to analyze with accuracy the small-angle anisotropic scattering and to determine the components of the radius of gyration $R_{\parallel}$ and $R_{\perp}$, the Guinier conditions $R_{\parallel} q \leqslant 1$, $R_{\perp} q \leqslant 1$ must be fulfilled. So the wavelength λ has been increased toward values between 10 and 15 Å in order to reach a domain of q values between 5×10^{-3} and 5×10^{-2} Å^{-1} mapped by the 2D multidetector (Fig. 5a and 5b).

At higher temperature, in the nematic phase, the anisotropy of the small-angle scattered intensity remains present, but is much weaker:

$$R_{\parallel} < R_{\perp}$$

These results on the anisotropy of the backbone conformation are observed on all the studied samples. So, in a simple scheme, one can imagine that whather the compound, the backbone is mainly perpendicular to its hanging moieties and it is more or less confined between smectic layers. This kind of anisotropy, although smaller, already exists in the nematic phase. Moreover, a diffuse scattering located at what will be the Bragg peak position in the smectic phase is always measured; it is the signature of smectic fluctuations in the nematic phase. In the case of PMA-CN, in the smectic phase, the Bragg peak is not measured at the same position. The deduced thickness of the smectic layers of about 35 Å is greater than the length of the mesogenic molecules. It can be concluded that a partial overlapping of mesogens occurs, due to the cyano dipole interactions. This type of smectic phase is named SmAd; in the nematic phase, one has measured also diffuse scattering, which is a proof of short-range smectic order.

When possible, the temperature behavior of both radius of gyration components has been studied especially in smectic phase, which usually exists over wide temperature range, which is not the case for the nematic phase. These results are reported on Fig. 7. They are a little different according to the compound studied. Although backbone anisotropy is always in the same direction $R_\perp > R_{||}$, the temperature behavior of both radius of gyration components is not the same for the several studied LCP. This will be discussed in Section 4. Let us see what is predicted by theories on the conformation of the backbone and on its thermal evolution.

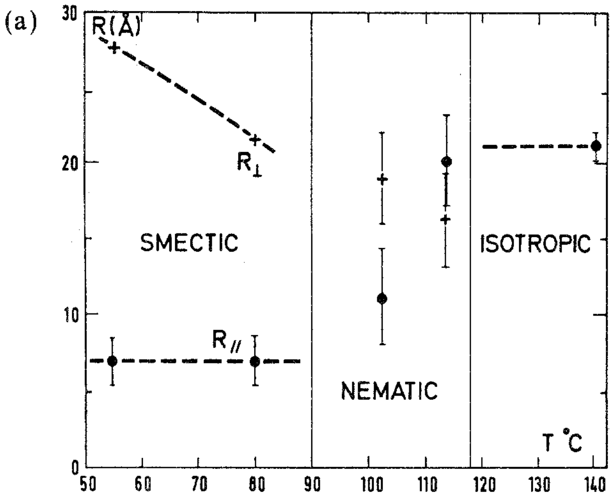

PA - OCH$_3$

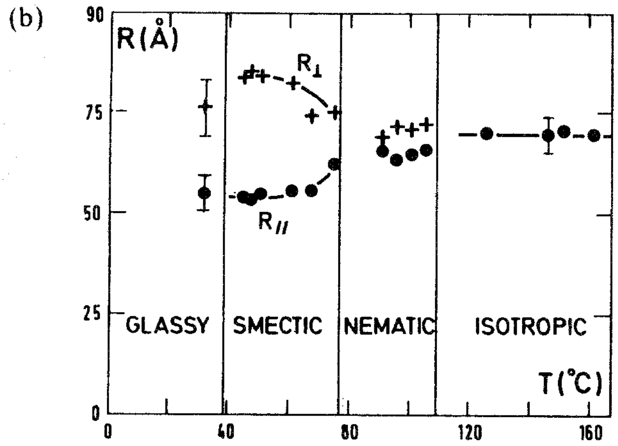

PMA - OCH$_3$

Fig. 7. Temperature dependence of $R_{||}$ and $R_\perp$ for four compounds (see the text). Broken and solid lines are guides for the eye.

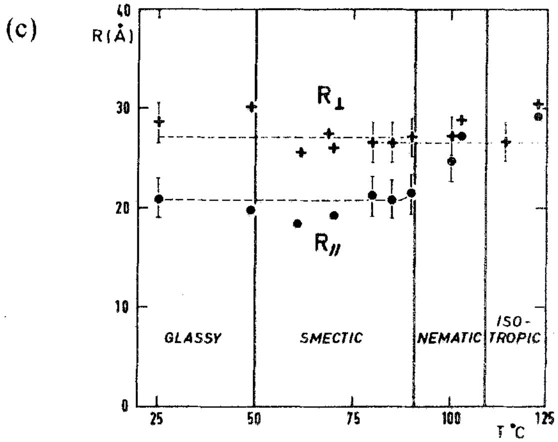

PMA - CN

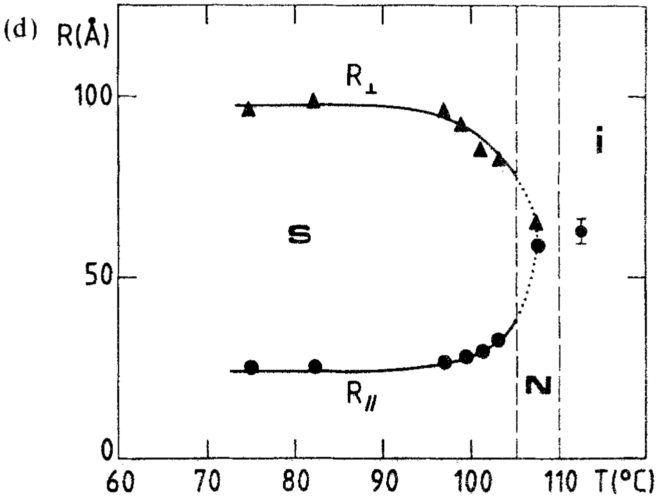

PMA - OC$_4$H$_9$

Fig. 7. (*Continued*)

3. REVIEW OF EXISTING THEORIES ON LCP

3.1. Conformation of LCP in Nematic Phase

3.1.1. Model Proposed by Wang and Warner.(11) Wang and Warner,[11] by solving standard diffusion equations, predict different conformations of the LCP backbone according to the values of parameters of their theory. The authors define four interactions: between backbones, between mesogenic cores, between backbone and spacer, and between mesogenic core and backbone. A fifth important parameter is the volumic ratio between backbone and grafted moieties. In order to compare with experiments, we select two main results of the Wang and Warner theory:

If the coupling between backbone and spacer is weak, the backbone lies more or less parallel to the nematic director, and has the shape of a prolate ellipsoid; on the contrary, if the repulsion between backbone and spacer is large, the backbone is perpendicular to the spacer and to the long axis of the mesogen, and has the shape of an oblate ellipsoid. Moreover, the authors calculate temperature dependence laws of $R_{\parallel}$ and $R_{\perp}$:

$$R_{\parallel}^2 \propto LT \qquad \text{and} \qquad R_{\perp}^2 \propto L/T$$

where L is the total length of the polymer.

3.1.2. Model Proposed by Vasilenko, Shibaev, and Khokhlov.(12) This model is based upon a derivation of Flory's model: a semiflexible chain applied on a cubic lattice. The main parameter in this model is once more the fraction of sites occupied by mesogens compared to the number of sites occupied by the backbone. According to the values taken by this parameter, different types of nematic phases appear. In this model no temperature behavior of the backbone conformation is predicted; backbone and mesogenic cores interact only by the mean of steric effects and of excluded volume.

3.2. Conformation of Polymer in the Smectic Phase

3.2.1. Model Proposed by Renz and Warner.(13) Renz and Warner(13) assume that the smectic phase order obliges the backbone to be confined between layers. However, the backbone can move along the director direction (that is, parallel to the long axis of mesogens) only by elementary step (hopping model) (Fig. 8). These jumps from one layer to another may be considered as defects. They are thermally activated, so the gyration radius component parallel to the director is given by an Arrhenius law:

$$R_{\parallel}^2 \propto \exp(-E/kT)$$

3.2.2. Model Proposed by Rieger.(14) Rieger considers that in the smectic phase backbones are stuck between smectic layers and each time one backbone goes through a layer, it costs energy, and the smectic

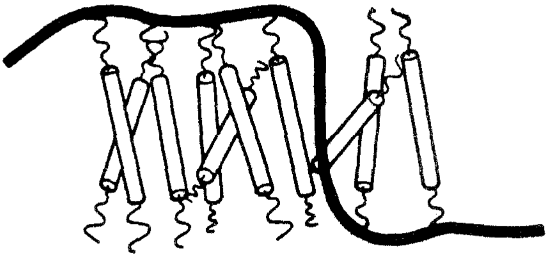

Fig. 8. The backbone of the LCP is mostly confined between two smectic layers of SmA1 type.

order in a layer is disturbed. So, as in Renz and Warner's model, it is found that

$$R_{\parallel}^2 \propto \exp(-E/kT)$$

The model gives also the conformation of LCP in the perpendicular direction. The evolution with temperature of $R_{\perp}$ depends on the assumptions made on the backbone:

If the backbone is considered as completely "free" (Gaussian walk) in a plane parallel to the smectic layers, $R_{\perp}$ is nearly constant with temperature.

If the backbone is rigid and can be considered as a stick, then $R_{\perp}$ is given by $R_{\perp}^2 \propto \exp(+E/kT)$.

3.2.3. Model Proposed by Dowell.(15,16) Dowell(15) proposes a model based upon *ab initio* calculations. All physical and chemical interaction parameters between the different parts of LCP are introduced in the model, such as dipole–dipole interaction, chemical bond potential, and so on; the model predicts a great number of properties of LCP, such as transition temperatures between liquid crystal phases, gyration radius components, and the tendency in the nematic phase for some LCP to form smectic fluctuations, and some of them have been found in agreement with experimental results.(16)

4. DISCUSSION

4.1. Smectic Phase

A strong anisotropy in the conformation of the backbone of LCP has been measured by mean of SANS and found always in the same direction: $R_{\perp} > R_{\parallel}$ for all the studied polymers. So, in the competition, smectic order is predominant and the backbone lies perpendicular to its hanging molecules.

In this section we compare our experimental results to theoretical models which predict a temperature behavior of both components of the radius of gyration.

If one fits the results of PMA-OC$_4$H$_9$ and PMA-OCH$_3$, following Renz and Warner,(13) with an Arrhenius law for $R_{\|}^2$, one finds an activation energy $E = 1$ eV (100 kJ/mole) (Fig. 9a). While $R_{\|}$ decreases with the temperature, $R_{\perp}$ increases in the same conditions for these two compounds (Fig. 7). Following Rieger's model, it might be an indication that the backbones become rigid as temperature is lowered. However, it must be also noticed that the variation of $R_{\|}$ can be fairly well described by a power law of the following type (Fig. 9b):

$$R_{\|} \propto (T_c - T)^{\alpha} \tag{8}$$

where T_c is the nematic–smectic transition temperature.

The value found for the exponent α is not a particular known value. But such a power law leads us think that a possible explanation of the

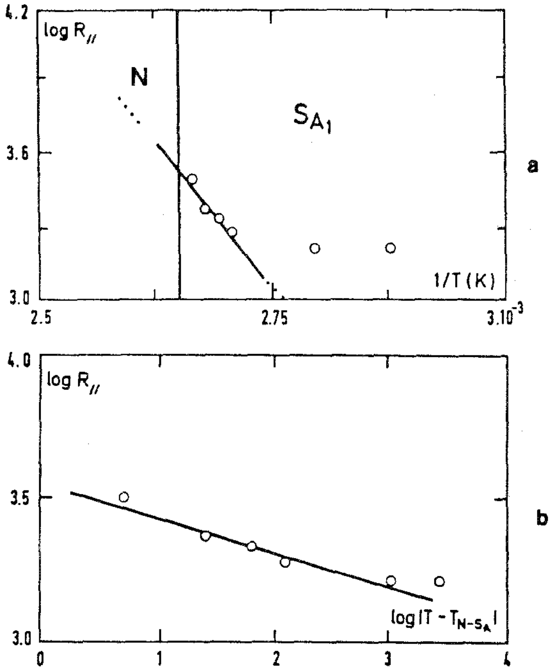

Fig. 9. Fits of $R_{\|}$ for PMA-OC$_4$H$_9$ (ref. 6): (a) by an Arrhenius law $R_{\|} \propto \exp(-E/2kT)$ with $E \approx 1$ eV; (b) by a power law $R_{\|} \propto (T - 105)^{-0.12 \pm 0.02}$.

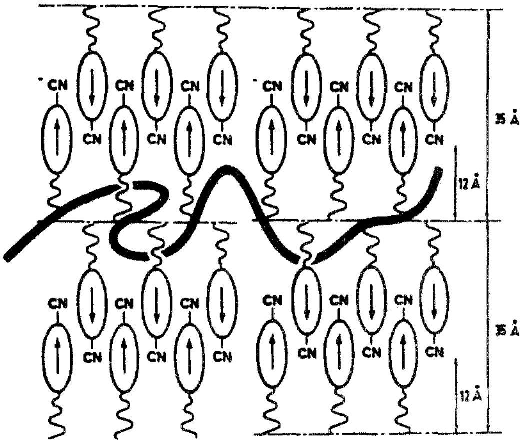

Fig. 10. A possible explanation of the temperature behavior of $R_\perp$ in PMA-CN: while in the SmA1 smectic phase $R_\perp$ increases with smectic order, in the SmAd smectic phase, $R_\perp$ is much less sensitive to smectic order and does not vary with temperature.

different temperature behaviors of the backbone conformation lies in the nature of the smectic order. If mesogenic cores making up the smectic layers are well segregated, backbones are stuck tightly between layers and $R_\perp$ is very sensitive to strains imposed on the polymer during the variation of temperature; this is the situation developed in SmA_1-type smectic phases (PMA-OC_4H_9, PMA-OCH_3) (Fig. 8). On the other hand, in a smectic phase where mesogens interdigitate (SmAd), the smectic density wave is "softer," less "square"; the LCP backbone has more room and it is less sensitive to strains. So $R_\perp$ does not significantly change with temperature: this is what is observed for PMA-CN (Fig. 10). In this scheme, the thermal evolution of the backbone conformation in smectic phases could be explained by the temperature dependence of the strength which orders hanging mesogenic cores, that is, the smectic order parameter.

4.2. Nematic Phase

From neutron measurements, it is found that a weak anisotropy remains in the nematic phase. One always has $R_\perp \geqslant R_{||}$. This could correspond to the oblate ellipsoid of phase N_I in Wang and Warner's theory(11); however, the same explanation as that given above in the smectic phase holds for nematic phase, for one must recall that in this phase smectic fluctuations are measured just before the nematic–smectic transition. The only case where the backbone is parallel to its own mesogens has been found in a reentrant nematic phase of PA-CN,(17) but this peculiar case will be not discussed here; a more general discussion on a great variety of LCP is in preparation and will be published elsewhere.(18)

As a conclusion, one can assert that liquid crystal polymers are good examples of model systems with competitive fields. From neutron measurements, it appears that the details of liquid crystal order may be directly responsible for the conformation of the LCP backbone and of its temperature dependence, in the nematic phase as well as in the smectic phase. Maybe existing theories based on the diffusive properties of usual polymers do not take this feature enough into account.

REFERENCES

1. Proceeding of the International Conference on Liquid Crystal Polymers, *Mol. Cryst.* **153** (1987); **155** (1988).
2. P. G. de Gennes, *Scaling Concepts in Polymer Physics* (Cornell University Press, Ithaca, New York, 1979).
3. P. G. de Gennes, *The Physics of Liquid Crystals* (Oxford, 1975).
4. J. P. Cotton, D. Decker, H. Benoît, B. Farnoux, J. Higgins, G. Jannink, J. des Cloizeaux, R. Ober, and C. Picot, *Macromolecules* **7**:863 (1974).
5. A. Guinier and G. Fournet, *Small Angle X-Ray Scattering* (Wiley, 1955); B. H. Zimm, *J. Chem. Phys.* **16**:1093 (1948).
6. L. Noirez, Thesis, Université Orsay, France (1989) [in French].
7. P. Keller, B. Carvalho, J. P. Cotton, M. Lambert, F. Moussa, and G. Pépy, *J. Phys. Lett.* **46**:L1065 (1985).
8. F. Hardouin, L. Noirez, P. Keller, M. Lambert, F. Moussa, and G. Pépy, *Mol. Cryst. Liq. Cryst.* **155**:389 (1988).
9. F. Moussa, J. P. Cotton, F. Hardouin, P. Keller, M. Lambert, G. Pépy, M. Mauzac, and H. Richard, *J. Phys.* (Paris) **48**:1079 (1987).
10. L. Noirez, J. P. Cotton, F. Hardouin, P. Keller, F. Moussa, G. Pépy, and C. Strazielle, *Macromolecules* **21**:1889 (1988).
11. X. J. Wang and M. Warner, *J. Phys. A Math. Gen.* **20**:713 (1987).
12. S. V. Vasilenko, V. P. Shibaev, and A. R. Khokhlov, *Makromol. Chem.* **186**:1951 (1985).
13. W. Renz and M. Warner, *Phys. Rev. Lett.* **56**:1268 (1986).
14. J. Rieger, *J. Phys.* (Paris) **49**:1615 (1988).
15. F. Dowell, *Mol. Cryst. Liq. Cryst.* **157**:203 (1988); **155**:457 (1988).
16. F. Dowell, *J. Chem. Phys.* **91**:1316, 1326 (1989).
17. L. Noirez, P. Keller, P. Davidson, F. Hardouin, and J. P. Cotton, *J. Phys.* (Paris) **49**:1993 (1988).
18. L. Noirez, to be published.